Strengthening of a 12CrMoV Turbine Blade Steel by Retempering

R.N. Singh, R. Kishore, G.K. Dey, I.S. Batra, and P. Dasgupta

Commercially available martensitic 12CrMo, 12CrMoV, and 12CrMoVNb steels in the tempered condition are often used to fabricate turbine blades. Tempering, done at the processing stage itself, is usually carried out at a temperature approximately 100 to 150 °C above the service temperature. At the service temperature, the steel undergoes a second tempering. The effect of this second tempering at a lower temperature on the strength of 12CrMoV steel is delineated and discussed in this paper.

Keywords
12CrMoV steel, microstructure, strengthening, tempering resistance, tensile properties, turbine blade

1. Introduction

MARTENSITIC 12 wt% Cr stainless steels that contain about 0.1 wt% C and small additions of molybdenum (1 to 1.5 wt%), vanadium (0.25 to 0.5 wt%), and sometimes niobium (0.1 to 0.3 wt%) are extensively used for high-temperature, creep-resistant applications (Ref 1, 2), including turbine blades. These steels are austenitic at 1000 to 1050 °C and, because of their high hardenability, transform martensite even upon air cooling. To produce useful combinations of strength, ductility, and toughness, these steels are usually tempered at temperatures 100 to 150 °C higher than the temperature at which these steels are likely to be used (Ref 2).

Molybdenum and vanadium are added to 12% Cr steels to improve tempering resistance and strength (Ref 3). Because these two elements are ferrite stabilizers, they tend to produce δ-ferrite when the steel is austenitized at 1050 °C. This δ-ferrite tends to reduce the strength of martensite that is obtained upon cooling after austenitization. To counteract the tendency of these steels to δ-ferrite formation due to the presence of molybdenum and vanadium, the constitution of these steels is usually balanced (Ref 3, 4) by nickel, which is known to be a γ-stabilizer. A constitutionally balanced steel is fully austenitic at the conventional austenitization temperature of 1050 °C. Upon air cooling, it transforms to a fully martensitic structure, which can then be tempered to obtain the optimum combination of strength, ductility, and toughness.

Niobium is sometimes added to 12CrMoV steels to further improve high-temperature creep resistance. Niobium behaves differently from molybdenum and vanadium because it combines with carbon to form niobium carbide, which is stable at the conventional austenitizing temperature of 1050 °C. Thus, apart from being a ferrite stabilizer, it also scavenges carbon (and nitrogen) from solution in steel. Because of this fact, constitutional balance for niobium is usually done by nickel (Ref 3, 5). In a constitutionally balanced 12CrMoVNb steel, the avail-

ability of less carbon in solution in austenite at 1050 °C affects the strength of martensite that is produced upon cooling. However, because the niobium-containing steels possess higher tempering resistance than those that contain only molybdenum and vanadium, niobium is added when the steel is likely to experience higher service temperatures.

Martensitic steels of the 12 wt% Cr variety are available commercially in the tempered condition only (Ref 2). The se-
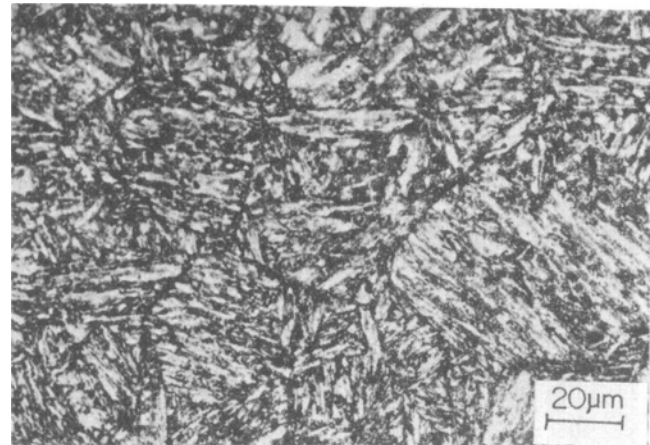

Fig. 1 Optical micrograph of the as-received (single-tempered) steel
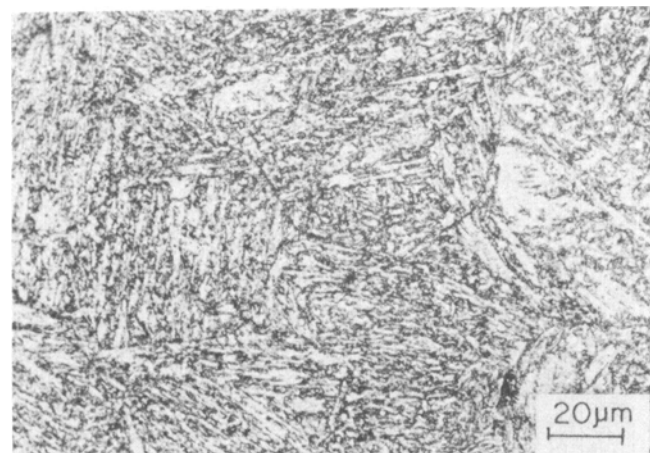

Fig. 2 Optical micrograph of the double-tempered steel

R.N. Singh, R. Kishore, G.K. Dey, I.S. Batra, and P. Dasgupta, Metallurgy Division, Bhabha Atomic Research Centre, Trombay, Bombay 400 085, India

quence of carbide precipitation at various tempering temperatures; the nature, composition, and morphology of carbides; and the structure/property correlations have been investigated in martensitic 12% Cr steels (Ref 6- 8). It is also known (Ref 9) that available tempered 12% Cr steels can be further strength-ened by a second tempering at a lower temperature. In the present work, as-received (tempered) 12CrMoV steel intended for turbine blade applications was characterized, and the effect of a second tempering carried out at 480 °C—the temperature at which the steel is used—was examined.
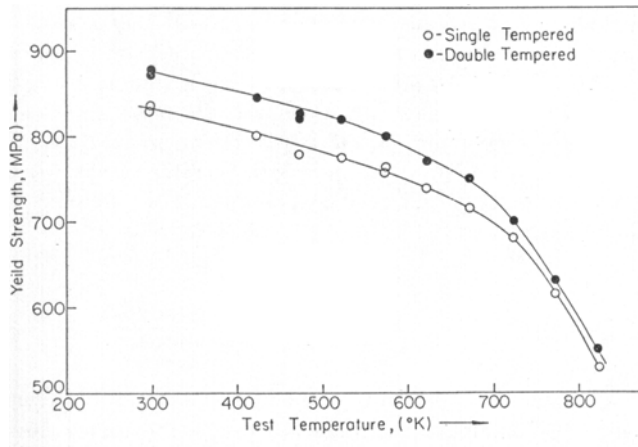
2. Experimental Details

The steel used in the present investigation had the following composition: Fe-0.14C-12.06Cr-1.56Mo-0.66V-2.33Ni-0.67Mn-0.017Si-0.03P-0.02S. It was received in the tempered martensitic condition (hardness, 34 HRC) in the form of a bar with a 120 by 120 mm cross section. Cylindrical tensile specimens with a gage length of 25 mm and a diameter of 6.25 mm were cut, the axes of the samples being in the transverse direction of the bar. To study the effect of a second tempering, some of the tensile samples were tempered at 480 °C for 48 h.

Samples from both the as-received stock and those that had been given a second tempering treatment were tensile tested on an automated servohydraulic tensile testing machine. Tensile tests were carried out in a temperature range of 298 to 823 K by employing a strain rate of 10^{-4}/s. Before the test began, the

Fig. 3 Variation in yield strength as a function of test temperature for the single-tempered and the double-tempered steels
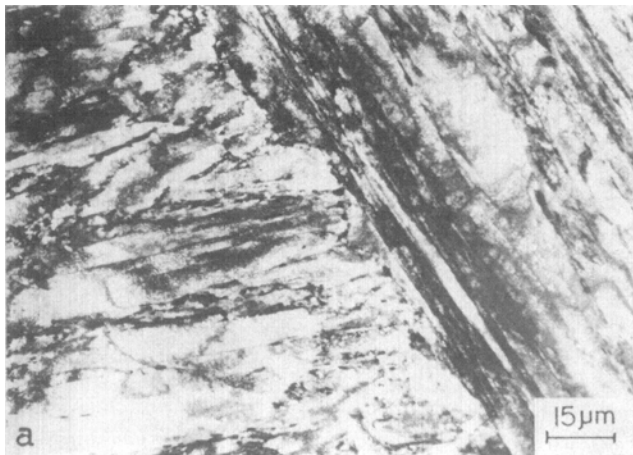

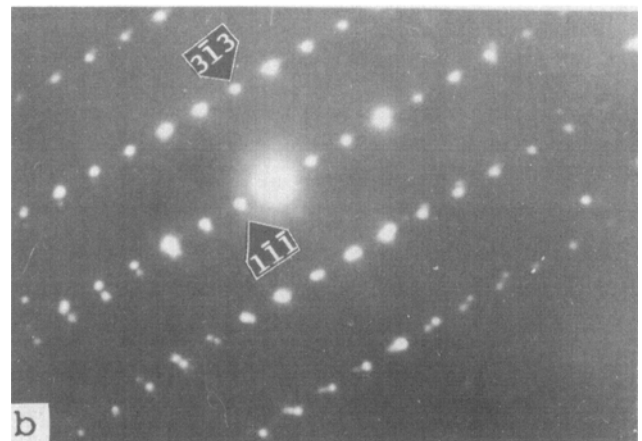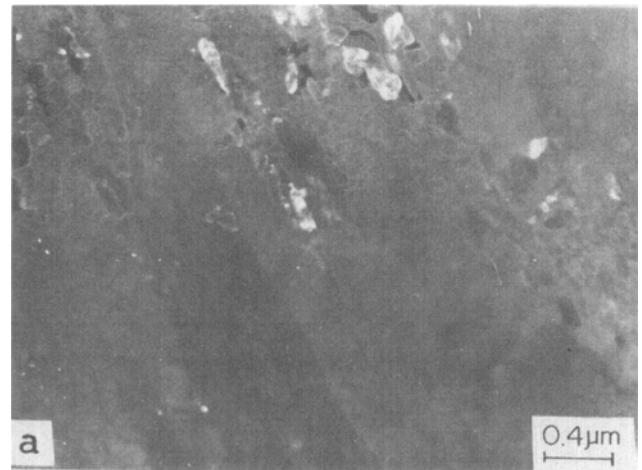Fig. 4 Bright-field TEM micrographs of the single-tempered steel

Fig. 5 (a) Dark-field TEM micrograph showing $M_{23}C_6$-type carbides. (b) Selected-area diffraction pattern showing spots due to $M_{23}C_6$ in the single-tempered steel. $M_{23}C_6$ zone axis $[\bar{2}\ \bar{3}1]$

sample and the grips were soaked at temperature for an hour to allow them to attain the test temperature. Load-elongation data were collected through an on-line computer and processed to give the stress-strain curves and the values of yield strength.
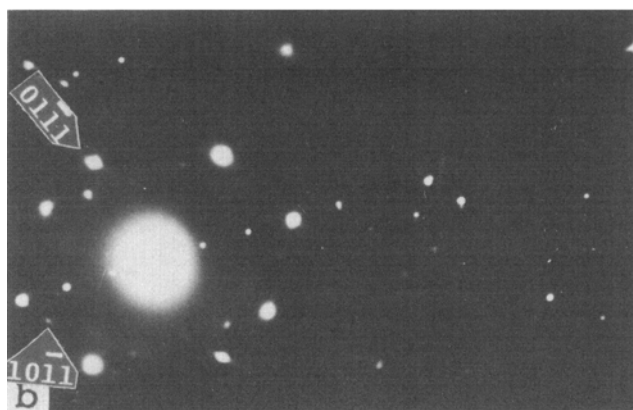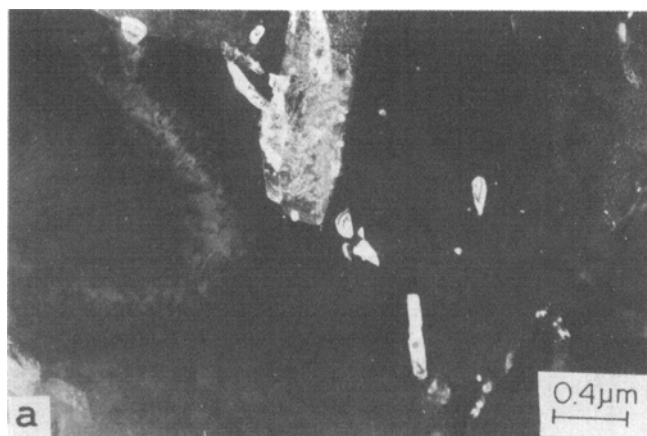

Fig. 6 (a) Bright-field TEM micrograph showing Cr_2N (or Fe_2C). (b) Selected-area diffraction pattern showing spots due to Cr_2N (or Fe_2C) in the single-tempered steel. Cr_2N zone axis $[1\bar{1}\bar{1}23]$
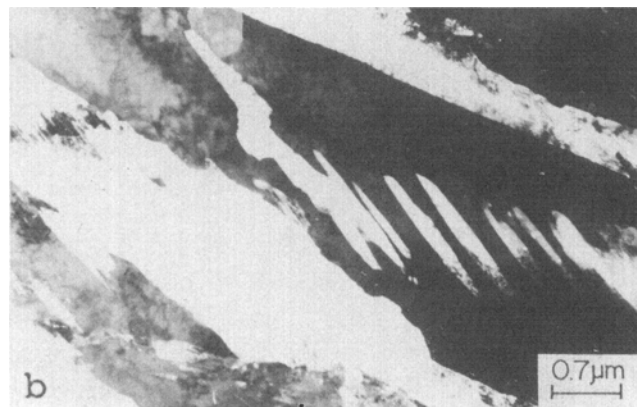
The microstructure of the steel in both the single-tempered (as-received) and the double-tempered (as-received + 480 °C/48 h) conditions was characterized by optical microscopy. To characterize the microstructural features in the as-received stock and to further investigate the effect of a second tempering on these features, transmission electron microscopy (TEM) was employed. For this purpose, thin slices were cut from the single-tempered and the double-tempered steels and were mechanically polished to a thickness of less than 100 µm. Further thinning was done by the window thinning technique, using a bath of 1:6:10 perchloric acid, n-butanol, and methanol maintained at a temperature of –30 °C. Electrochemical thinning was carried out at 20 V. To identify the various carbides and other fine particles, extensive selected-area diffractometry (SAD) was performed.

3. Results

As shown in Fig. 1, the as-received steel was in a tempered martensitic condition. The microstructure of the double-tempered steel is depicted in Fig. 2, which shows that the second tempering at the lower temperature of 480 °C for 48 h apparently did not alter the microstructure. The hardness also did not change significantly. However, the tensile properties of the steel subjected to the double-tempering treatment were found to be different from those of the single-tempered steel. In Fig. 3, the variation in yield strength is plotted as a function of test temperature for both the single- and double-tempered steel. As a result of the second tempering, the steel was slightly strengthened, the extent of this strengthening decreasing with increasing test temperature. On the basis of the observed microstructures (Fig. 1 and 2), it was rather difficult to rationalize this fact. Therefore, thin-foil TEM was carried out to reveal the changes in the microstructural features as a result of the second tempering.

Figure 4 depicts bright-field TEM micrographs of the steel in the as-received condition. Apart from martensite laths, fine particles are visible at the boundaries between the laths as well as at the prior-austenite grain boundaries. These were indexed primarily as $M_{23}C_6$-type carbides. In the dark-field micrograph

Fig. 7 Bright-field (a) and dark-field (b) micrographs showing internally twinned plates in the single-tempered steel

depicted in Fig. 5(a), these carbides are shown from a different area of the foil at a higher magnification. The corresponding
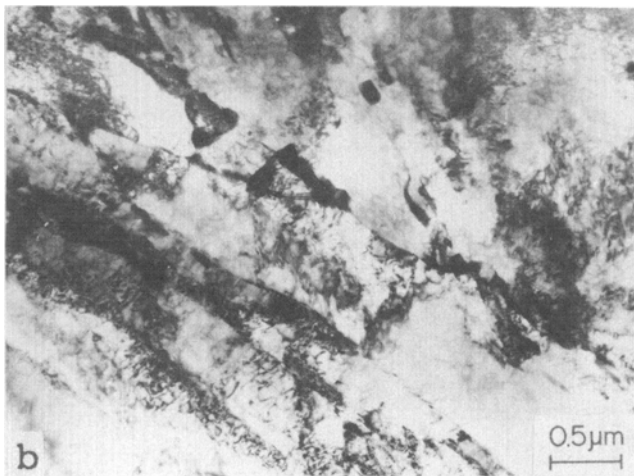

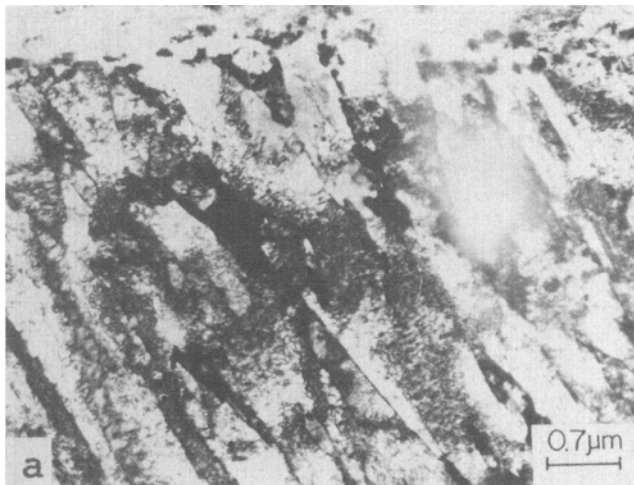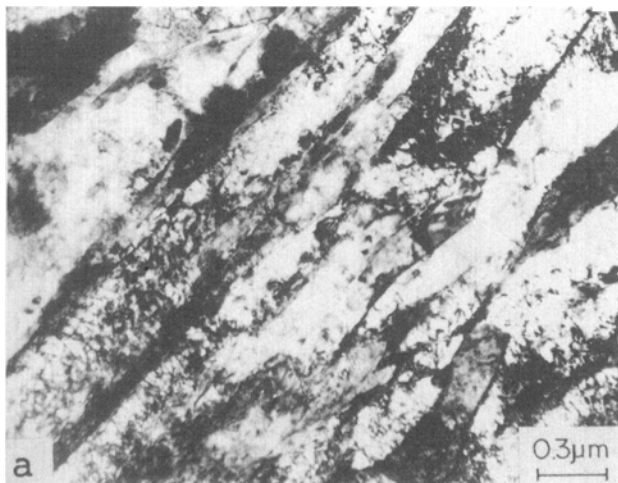**Fig. 8** Bright-field TEM micrographs showing dislocation networks in the single-tempered steel

Fig. 9 Bright-field TEM micrographs of the double-tempered steel

properly indexed SAD pattern showing spots due to $M_{23}C_6$-type carbides is depicted in Fig. 5(b). Occasionally some extremely fine particles could be indexed as Cr_2N or Fe_2C. A bright-field micrograph showing these particles and the corresponding SAD pattern are presented in Fig. 6. Apart from the above observations, some interesting features such as internally twinned plates (Fig. 7) and dense dislocation networks (Fig. 8) were also seen.

In the double-tempered steel (Fig. 9), all the fine-scale microstructural features were similar to those obtained in the as-received single-tempered steel. In this condition, the carbides also could be indexed as $M_{23}C_6$ type. However, a new feature was the development of Fe_2Mo (Fig. 10). There was no substantial change in the distribution of dislocations as a result of the second tempering (Fig. 11).

4. Discussion

The results relating to the characterization of the as-received single-tempered 12CrMoV turbine blade steel are in agreement with similar observations made earlier by others (Ref 6-9). The strengthening that results due to the second tempering at a lower temperature has also been a subject of discussion in the work of Irvine and Pickering (Ref 9). In their work, strengthening was attributed to the formation of a M_2C-type matrix carbide because all carbon was not used up for the formation of $M_{23}C_6$-type carbides at the higher temperature of the first tempering. Corresponding to the solubility limit of carbon at the first tempering temperature, carbon is left in solution. At the second (lower) tempering temperature, the solubility limit of carbon being lower, excess carbon precipitates out.

In the present work, however, precipitation of Fe_2Mo was observed as a result of the second tempering. Although justified by Irvine and Pickering (Ref 9), precipitation of M_2C-type carbides in the matrix cannot be responsible for changes in strength for both the short-time and long-time second tempering. This is because once the saturation in strengthening at the temperature corresponding to the second tempering is attained, tempering for longer times would not lead to additional
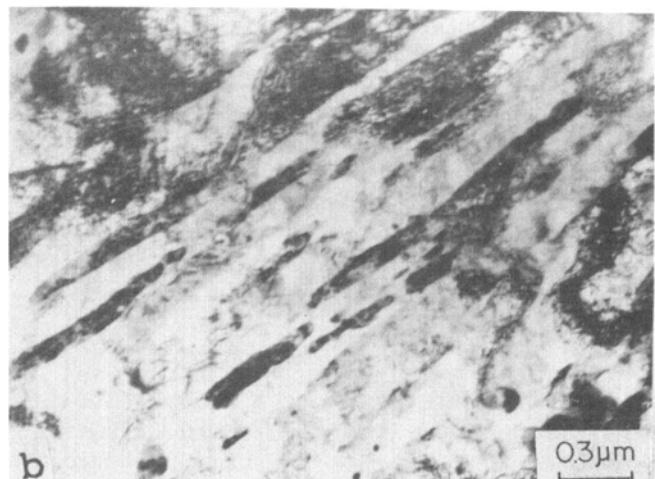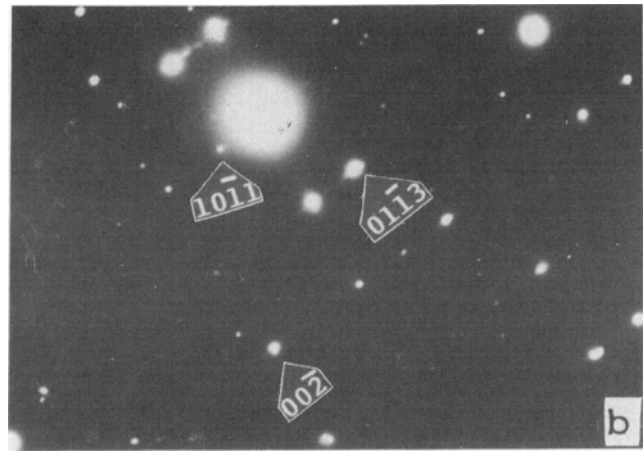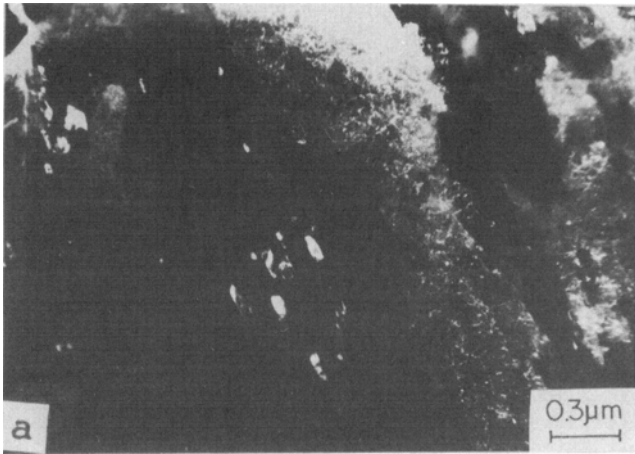
Fig. 10 (a) Dark-field TEM micrograph showing Fe_2Mo and $M_{23}C_6$-type carbides. (b) Selected-area diffraction pattern showing spots due to ferrite and Fe_2Mo in the double-tempered steel. Fe_2Mo zone axis [$\overline{5}7\overline{2}3$]
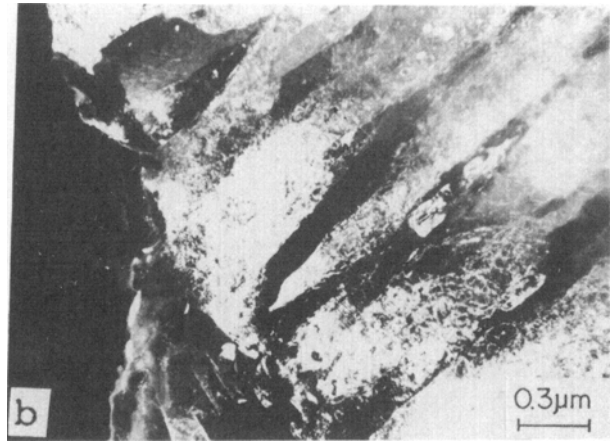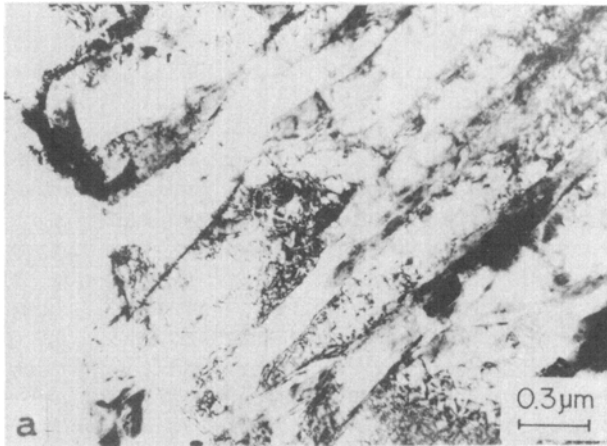

Fig. 11 Bright-field (a) and dark-field (b) TEM micrographs showing dislocation networks in the double-tempered steel

strengthening unless a new precipitate formed. Therefore, the strengthening observed in the present work as a result of the second tempering can be ascribed to the formation of Fe_2Mo.

The decrease in the extent of strengthening as the test temperature is increased may be due to the strengthening of the as-received stock that occurred while it was being soaked for testing. The higher the test temperature, the greater the strength achieved by the as-received stock during soaking and, therefore, the less the difference in the yield strength values of the as-received and the double-tempered materials.

5. Conclusions

The as-received single-tempered 12CrMoV steel was found to exhibit known tensile behavior. A second tempering of this steel at a lower temperature resulted in an increase in tensile strength. This was attributed to the formation of fine particles of intermetallic Fe_2Mo.

Acknowledgment

References

1. J.Z. Briggs and T.D. Parker, The Super 12% Cr Steels, *Source Book of Materials for Elevated Temperature Applications,* Ed. E.F. Bradley, American Society for Metals, Metals Park, OH, 1979, p 92-177

2. *Metals Handbook,* 9th Edition, Vol 3 and 4, American Society for Metals, Metals Park, OH, 1980

3. K.J. Irvine, D.J. Crowe, and F.B. Pickering, The Physical Metallurgy of 12% Cr Steels, *The Metallurgical Evolution of Stainless Steels,* Ed. F.B. Pickering, American Society for Metals, Metals Park, OH and The Metals Society, London, England, 1979, p 43-62

4. T. Marrison and A. Hogg, Influence of Nickel Content on the Structure and High Temperature Properties of a 12% Cr-Mo-Nb Steel, *Creep Strength in Steel and High Temperature Alloys,* Ed. J. Nutting, The Metals Society, Sheffield, England, 1972, p 242-248

5. F.B. Pickering, Introduction, *The Metallurgical Evolution of Stainless Steels,* Ed. F.B. Pickering, American Society for Metals, Metals Park, OH and The Metals Society, London, England, 1979, p 1-42

6. J. Orr, F.R. Beckett, and G.D. Fawkes, The Physical Metallurgy of Cr-Mo Steels for Fast Reactor Boilers, *Ferritic Steels for Fast Reactor Stam Generators,* Ed. S.F. Pughand E.A. Little, BNES, London, England, 1978, p 91-109

7. M. Wall, Ph.D. Thesis, Imperial College, London, 1985

8. E.A. Little, D.R. Harries, F.B. Pickering, Some Aspects of the Structure Property Relationships in 12% Cr steels, *Ferritic Steels for Fast Reactor Steam Generators,* Ed. S.F. Pugh and E.A. Little, BNES, London, England, 1978, p 136-144

9. K.J. Irvine and F.B. Pickering, in F.B. Pickering, High Strength 12% Cr Steels, *The Metallurgical Evolution of Stainless Steels.* Ed. F.B. Pickering, American Society for Metals, Metals Park, OH and the Metals Society, London, England, 1979, p 63-77